# Piercing the Dirac spin liquid: From a single monopole to chiral states

Sasank Budaraju, Yasir Iqbal, Federico Becca, and Didier Poilblanc

Phys. Rev. B **108**, L201116 — Published 21 November 2023

DOI: 10.1103/PhysRevB.108.L201116

# Piercing the Dirac spin liquid: from a single monopole to chiral states

Sasank Budaraju,[1,2] Yasir Iqbal,[2] Federico Becca,[3] and Didier Poilblanc[1]

[1]*Laboratoire de Physique Théorique, Université de Toulouse, CNRS, UPS, France*
[2]*Department of Physics and Quantum Centre of Excellence for Diamond and Emergent Materials (QuCenDiEM), Indian Institute of Technology Madras, Chennai 600036, India*
[3]*Dipartimento di Fisica, Università di Trieste, Strada Costiera 11, I-34151 Trieste, Italy*

(Dated: November 2, 2023)

The parton approach for quantum spin liquids gives a transparent description of low-energy elementary excitations, e.g., spinons and emergent gauge-field fluctuations. The latter ones are directly coupled to the hopping/pairing of spinons. By using the fermionic representation of the $U(1)$ Dirac state on the kagome lattice and variational Monte Carlo techniques to include the Gutzwiller projection, we analyse the effect of modifying the gauge fields in the spinon kinematics. In particular, we construct low-energy monopole excitations, which are shown to be gapless in the thermodynamic limit. States with a finite number of monopoles or with a finite density of them are also considered, with different patterns of the gauge fluxes. We show that these chiral states are not stabilized in the Heisenberg model with nearest-neighbor super-exchange couplings, and the Dirac state corresponds to the lowest-energy *Ansatz* within this family of variational wave functions. Our results support the idea that spinons with a gapless conical spectrum coexist with gapless monopole excitations, even for the spin-1/2 case.

*Introduction.* Quantum spin models on frustrated low-dimensional lattices represent a playground to investigate a variety of different phases of matter and the transitions among them [1]. Even though a full characterization of their phase diagrams would require a finite-temperature analysis, in most cases the knowledge of the ground state and a few low-energy excitations is enough to obtain important information on the relevant (low-temperature) behavior. Still, achieving an accurate description of the exact ground state of frustrated spin models poses itself as a difficult task. Indeed, a faithful characterization can be obtained whenever (a sizable) magnetic order is present, since here the ground state is well approximated by a product state, with spins having well-defined expectation values on each site. By contrast, whenever magnetic order is significantly suppressed, or even absent, the ground-state wave function is much more elusive. The most complicated case is given by the so-called quantum spin liquids, where the elementary degrees of freedom are no longer the original spin variables, but emergent particles (spinons) and gauge fields (visons or magnetic monopoles) [2]. The standard approach to describe spin liquids is through the parton construction, where spin operators are represented by using fermionic or bosonic particles; here, the original Hilbert space is enlarged and additional gauge fields are introduced [3–5]. Thus, the resulting model describes fermions or bosons that interact through gauge fields on a lattice. A spin liquid corresponds to the deconfined phase of the resulting model, in which particles (spinons) are free at low energies. In this case, the elementary excitations of the spin model are fractionalized, i.e., they are not integer multiples of those of the original constituents. By contrast, whenever the gauge fields lead to confinement, the spin liquid is unstable towards some symmetry-breaking phenomenon, most notably the establishment of valence-bond or magnetic order [6]. The analysis of these lattice gauge theories is not easy and requires non-perturbative methods [7–9], which also include a detailed examination of the symmetries of low-energy excitations. Still, some insight can be obtained from mean-field approaches [10], where gauge fields are frozen and fermions/bosons are free. From there, it is also possible to extract some information on the nature of the most relevant gauge fluctuations: whenever they are gapped (corresponding to a $\mathbb{Z}_2$ symmetry) the low-energy spectrum of the spinons is not qualitatively modified, leading to stable $\mathbb{Z}_2$ spin liquids [10] (the most remarkable example being the Kitaev model on the honeycomb lattice [11]). The situation is more delicate when the low-energy gauge fields are gapless (with $U(1)$ symmetry), since in this case they can spoil the mean-field properties of the spinon spectrum. In particular, monopoles proliferate and may give rise to a confined phase [12]. Still, the presence of a sufficiently large number of massless fermions may screen the monopoles and prevent confinement [7, 13, 14].

Among various possibilities, the nearest-neighbor $S = 1/2$ Heisenberg antiferromagnetic model on the kagome lattice represents one of the most intriguing and important examples in which magnetic frustration may give rise to a non-magnetic ground state. The interest in this spin model was raised after the discovery of a number of compounds, where localized $S = 1/2$ moments interact through a super-exchange mechanism in almost decoupled kagome layers. The most notable example is given by the so-called Herbertsmithite $Cu_3Zn(OH)_6Cl_2$ [15–17]. Here, there is no evidence of magnetic order down to extremely small temperatures, thus suggesting the possibility that the ground state is indeed a quantum spin liquid [18]. Triggered by these outcomes, a huge effort has been spent in the last years to clarify the actual nature of the ground state of the Heisenberg model on the kagome lattice. Early large-scale density-matrix renormalization group (DMRG) calculations suggested the existence of a gapped spin liquid [19, 20], while variational Monte Carlo techniques, more recent DMRG and tensor network approaches, and pseudo-fermion functional renormalization

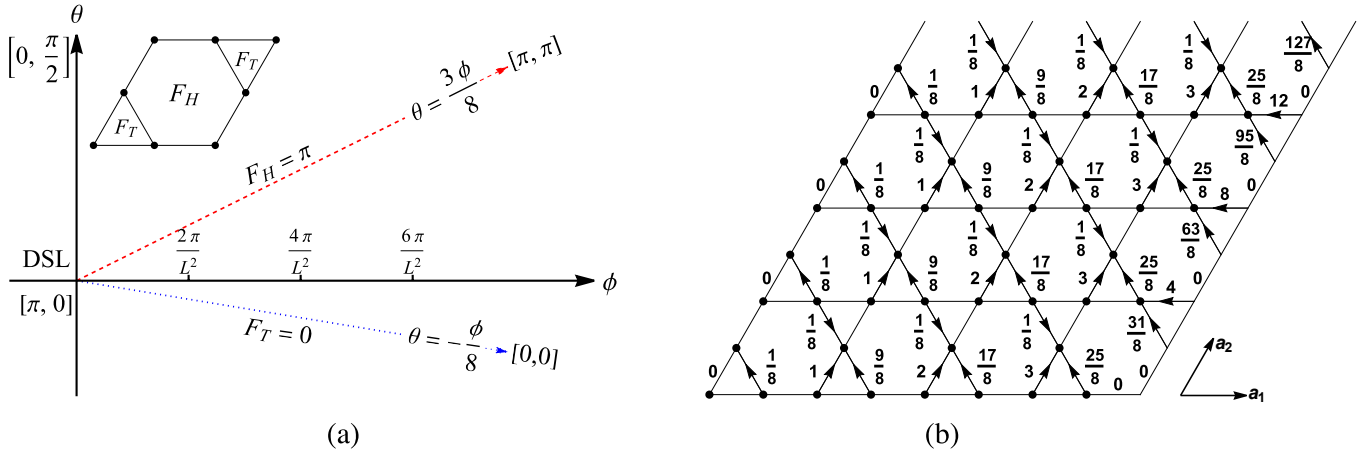


FIG. 1. (a) The plane $(\phi, \theta)$ that defines the flux distribution in the unit cell considered in this work, shown in the inset. The hexagonal plaquette has a $F_H = \pi - 2\theta + 3\phi/4$ and two triangular ones have flux $F_T = \phi/8 + \theta$. The $[\pi, 0]$ Dirac state lies at the origin, the uniform state $[0, 0]$ is obtained with $\theta = -\phi/8$ for $\phi = \pm\pi$, and the $[\pi, \pi]$ state with $\theta = 3\phi/8$ and $\phi = 2\pi$. The quantized values of $\phi$, obtained for a few monopoles are marked on the $x$-axis. (b) The complex argument $\alpha_{i,j}$, in units of $2\pi/L^2 = 2\pi/16$, of the hopping parameters $e^{\mathrm{i}\alpha_{i,j}}$ (for $i \to j$) and $e^{-\mathrm{i}\alpha_{i,j}}$ (for $j \to i$) of the fermionic Hamiltonian (3) that defines a single-monopole configuration (with $\theta = 0$) on the $L = 4$ cluster. Notice that the translational symmetry is broken by the hoppings on the rightmost column along $\mathbf{a}_2$.

group calculations supported a gapless spin liquid [21–25]. The variational approach has a very simple and elegant description within the fermionic parton representation; here, the free fermions have only kinetic terms (no pairing), defining peculiar magnetic fluxes piercing the unit cell (i.e., $\pi$-flux through hexagonal plaquettes and 0-flux through triangular ones), thus leading to two Dirac points in the spinon spectrum [21, 26]. As a consequence, this *Ansatz* is dubbed as $[\pi, 0]$ Dirac spin liquid. Finally, an accurate variational wave function is obtained by including the Gutzwiller projection, which imposes a single-fermion occupation on each lattice site [21, 22].

Still, alternative scenarios have been proposed, the most intriguing one suggesting the possibility that the ground state is a chiral spin liquid [28, 29], which break time-reversal and point-group symmetries [30]. Originally, chiral spin liquids have been constructed in analogy to the fractional quantum Hall effect [31]. However, the main difference with respect to the latter case is that time-reversal is spontaneously broken, leading to even more exotic phenomena [32]. Recently, different calculations suggested that chiral spin liquids may exist in extended Heisenberg models on the kagome lattice, e.g., adding super-exchange couplings at second or third neighbors, multi-spin interactions, or Dzyaloshinskii-Moriya terms [33–42]. In addition, chiral spin liquids have been also analysed within mean-field approaches, in terms of both bosonic [43, 44] and fermionic partons [32, 45].

In this paper, we study the stability of the Dirac spin liquid wave function, which has been proposed to capture the correct ground-state properties of the nearest-neighbor Heisenberg model on the kagome lattice [21, 22], against chiral perturbations. We analyse the energetics of Gutzwiller-projected fermionic states that are obtained by adding non-trivial magnetic fluxes to the ones that define the Dirac wave function. In particular, we can independently (i) consider an additional flux (parametrized by $\phi$ and spread uniformly on the lattice) and/or (ii) redistribute the flux inside the unit cell (parametrized by $\theta$); hence, we assume that every unit cell has the same distribution of fluxes in the hexagonal and triangular plaquettes, see Fig. 1. The flux through the triangular plaquettes is given by $F_T = \phi/8 + \theta$, while the flux through the hexagonal ones is $F_H = \pi - 2\theta + 3\phi/4$, such that the total flux piercing the unit cell is $F_C = \pi + \phi$, the Dirac state being recovered with $\phi = \theta = 0$. All calculations are performed on tori with $3 \times L \times L$ sites by using variational Monte Carlo techniques to assess the properties of the Gutzwiller-projected states [46]. On finite clusters, $\phi$ is quantized, while $\theta$ may assume any value. A "commensurate" flux $\phi = 2\pi/q$ requires a large super-cell that includes $q$ unit cells (assuming $q$ divides $L$) and implies a total flux multiple of $2\pi L$ on the whole torus. In addition to these standard cases, we also consider monopole configurations. A single monopole brings a $2\pi$ flux on the torus, thus leading to $\phi = 2\pi/L^2$ on each unit cell; states with $N_{\mathrm{mp}}$ monopoles are then constructed by considering a flux density $\phi = 2\pi N_{\mathrm{mp}}/L^2$. On the one hand, this allows us to study the energetics of a single monopole on finite clusters and its scaling in the thermodynamic limit; on the other hand, with monopole configurations, the stability of the Dirac state may be assessed for very small additional fluxes (i.e., much smaller than the minimal one accessible within the commensurate fluxes). The main outcome of this study is that the Dirac state is stable against chiral perturbations. Still, monopole excitations are gapless in the thermodynamic limit. We would like to emphasize that, since we work on tori, the analysis of the monopole energy cannot be directly connected to the scaling dimensions, as usually done within conformal-field theories, which consider a spherical geometry [13, 14, 47, 48].

*Model and methods.* We study the Heisenberg model on the kagome lattice with nearest-neighbor super-exchange interaction $J > 0$

$$\mathcal{H} = J \sum_{\langle i,j \rangle} \mathbf{S}_i \cdot \mathbf{S}_j, \tag{1}$$

where $\mathbf{S}_i = (S_i^x, S_i^y, S_i^z)$ is the spin-1/2 operator on a site $i$; periodic-boundary conditions are assumed on a cluster with $3 \times L \times L$ sites. In the following, we fix $J = 1$.

The variational wave functions are defined by

$$|\Psi\rangle = \mathcal{P}_G |\Phi_0\rangle, \tag{2}$$

where $|\Phi_0\rangle$ is the ground state of the auxiliary (non-interacting) Hamiltonian:

$$\mathcal{H}_0 = \sum_{\langle i,j \rangle, \sigma} \chi_{i,j} c_{i,\sigma}^\dagger c_{j,\sigma} + \text{h.c.}, \tag{3}$$

where $c_{i,\sigma}^\dagger$ ($c_{i,\sigma}$) creates (destroys) a fermion on site $i$ with spin $\sigma = \uparrow, \downarrow$; $\chi_{i,j} = \chi_{i,j}^0 e^{\mathrm{i}\alpha_{i,j}}$ defines the hopping amplitude for nearest-neighbor sites $(i, j)$. The "bare" term $\chi_{i,j}^0 = \pm 1$ defines the $[\pi, 0]$ flux pattern of the Dirac spin liquid, while the presence of $\alpha_{i,j} \neq 0$ allows us to consider $\theta \neq 0$ and/or $\phi \neq 0$ (including single- or multi-monopole states), see Fig. 1. In addition, periodic- or anti-periodic-boundary conditions can be taken in $\mathcal{H}_0$. In practice, the auxiliary Hamiltonian is diagonalized and $|\Phi_0\rangle$ is constructed as the Slater determinant of the lowest $N$ single-particle orbitals (where $N = 3L^2$), which is well defined whenever there is a closed shell configuration, i.e., a finite-size gap between the $N$-th and the $(N+1)$-th levels. For commensurate fluxes, we adopt the Landau gauge, which implies a $q \times 1$ super-cell. By contrast, the single-monopole configuration requires a super-cell as large as the entire cluster (which remains the case also for multi-monopole configurations). A similar monopole construction has been discussed in Ref. [49] for the square lattice. We remark that, whenever a single monopole is considered on top of the Dirac state, there is an exact degeneracy at the Fermi level (which is robust to changing the boundary conditions [50]), with two levels per spin, i.e. four levels occupied by two fermions giving rise to 6 monopoles (3 singlets and 1 triplet) [8, 51]. We verified that any occupation of these levels gives the same variational energy. In this case, the unprojected state $|\Phi_0\rangle$ does not correspond to a closed shell configuration and we use the single-particle orbitals obtained by the real-space diagonalization, without imposing any lattice symmetry. Then, monopole configurations do not correspond to specific $k$-points of the Brillouin zone.

Finally, $\mathcal{P}_G$ is the Gutzwiller projection onto the configuration space with one particle per site:

$$\mathcal{P}_G = \prod_i (n_{i,\uparrow} - n_{i,\downarrow})^2, \tag{4}$$

where $n_{i,\sigma} = c_{i,\sigma}^\dagger c_{i,\sigma}$. As a result, $|\Psi\rangle$ of Eq. (2) defines a faithful variational wave function for the spin Hamiltonian (1).

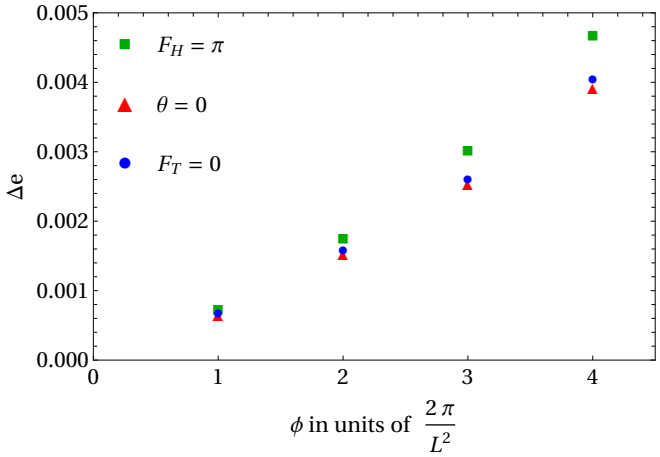


FIG. 2. Energy (per site) difference between chiral and Dirac states as a function of $\phi$ for three cuts in the plane of Fig. 1. Variational Monte Carlo calculations are performed on a cluster with $L = 8$. The values of $\phi$ correspond to $N_{\text{mp}} = 1, \ldots, 4$ monopoles in the torus.

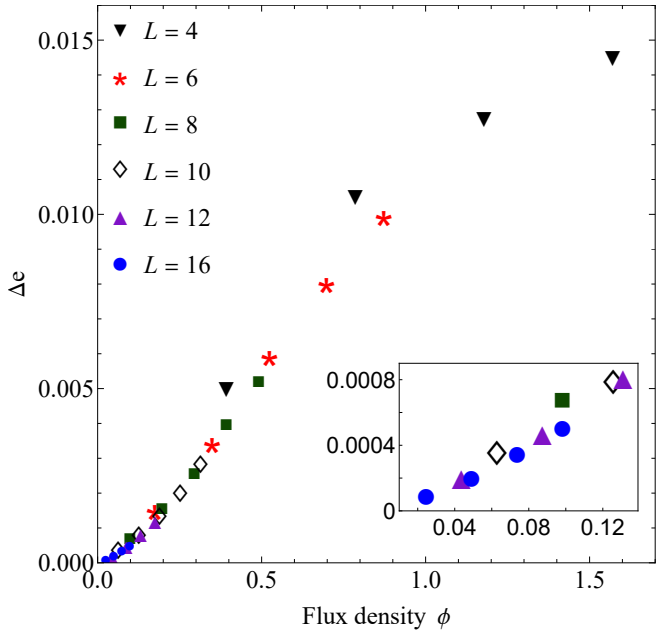


FIG. 3. Energy (per site) difference between chiral and Dirac states as a function of $\phi$ for $\theta = 0$, i.e., the x-axis of the plane shown in Fig. 1. The variational Monte Carlo calculations are done for both commensurate and monopole fluxes. Inset: zoom of the results for small values of $\phi$, where only monopole configurations are present.

Standard Monte Carlo sampling based upon Markov chains is used to evaluate the variational energy [46]. For the Hamiltonian (1), the Dirac state has an energy per site $e \approx -0.429$, which is higher than the best DMRG and tensor network estimates for the ground state, e.g, $e \approx -0.438$ [20, 24]. Still, this simple variational state may well capture the correct properties of the actual ground-state wave function, as suggested by recent DMRG calculations [23].

*Results.* The main outcome of this work is that the Dirac

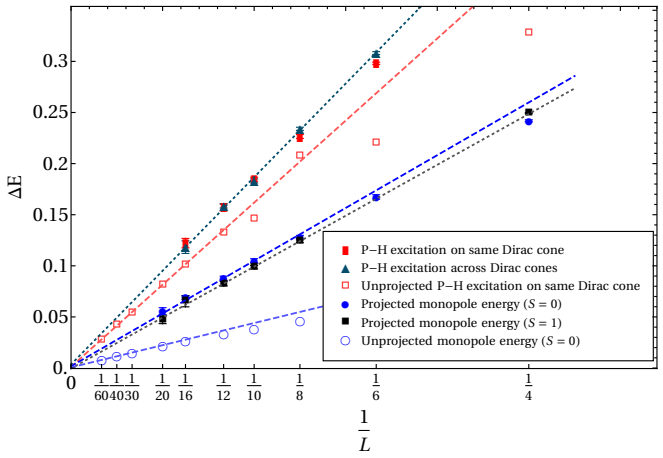


FIG. 4. Size scaling of the single-monopole gap (with respect to the Dirac state), both singlet and triplet cases are shown. The unprojected case (no Gutzwiller projection) is reported for comparison. Particle-hole (P-H) spinon excitations of the Dirac wave function are also shown, either within the same Dirac cone or across the Dirac cones.

state is stable when considering fluxes $\phi \neq 0$ and/or $\theta \neq 0$. Indeed, the best variational energy (per site) when varying $\theta$ and $\phi$ is obtained for $\theta = \phi = 0$, corresponding to the $[\pi, 0]$ case. As an example, in Fig. 2, the variational energies for different cuts in the $(\phi, \theta)$ plane are reported for $L = 8$: along $\theta = 3\phi/8$ (i.e., $F_H = \pi$, which connects the Dirac state to the $[\pi, \pi]$ one), along $\theta = -\phi/8$ (i.e., $F_T = 0$, which connects the Dirac state to the $[0, 0]$ one), and $\theta = 0$. In all cases, the energy increases with $\phi$, even for the smallest possible values obtained with a few monopoles. Similar results have been obtained for larger cluster sizes and different cuts. In particular, the case with $\theta = 0$ is reported in Fig. 3, where several sizes of the cluster are reported from $L = 4$ to $L = 16$, including both commensurate fluxes (the smallest one being $\phi = 2\pi/L$) and monopole configurations (which allow us to reach much smaller values of the fluxes). Our results clearly show that the minimal variational energy is always obtained with $\phi = 0$, i.e., for the Dirac state.

Next, we perform the explicit size-scaling analysis of the single-monopole gap, see Fig. 4. At the unprojected level, i.e., when the Gutzwiller projection of Eq. (4) is not imposed, the monopole configugration corresponds to an excited state that becomes gapless in the thermodynamic limit. Obviously, this result does not depend on the filling of the degenerate levels at the Fermi level, including the case where a triplet state is taken. We emphasize that the vanishing extrapolation becomes evident only when large clusters are considered (e.g., $L \gtrsim 30$), since a fitting procedure that only includes $L \lesssim 12$ would predict a finite gap for $L \to \infty$. Most importantly, the presence of the Gutzwiller projection has no effect on the overall behavior. In fact, while the slope of the fit is increased, the extrapolated value in the thermodynamic limit is always consistent (within a few errorbars) with a vanishing gap. In addition, there is no appreciable difference (for large clusters) between states with $S = 0$ (two fermions occupying orbitals at the Fermi level with up and down spins) or $S = 1$ (two fermions occupying the orbitals with the same spin). Note that, more generally, monopole excitations in the SU($N_f$) Heisenberg model [52] with $N_f$ even and $N_f/2 > 1$ fermions per site were also found to be gapless [50].

In order to prove (and improve) the statement that spinons are gapless, we construct particle-hole excitations of the Hamiltonian (3), by changing the fermion occupation in the unprojected state (i.e., by emptying one of the highest-energy single-particle orbital and filling one of the lowest-energy ones). Given the shape of the cluster, there are several ways to do this, since both these shells are four-fold degenerate (for each spin value). In particular, we can perform excitations within the same Dirac cone or across the two cones. Trivially, these states are gapless in the unprojected wave function, when $L \to \infty$. Most interestingly, they remain gapless even when the Gutzwiller projection is included. As a consequence, the $[\pi, 0]$ *Ansatz*, obtained from the auxiliary Hamiltonian (3) with *real* hoppings $\chi_{i,j} = \pm 1$, has the remarkable property to describe the (approximated) ground-state wave function that sustain gapless excitation for both spinons [53] and monopoles.

*Discussion.* In this work, we constructed monopole excitations on top of the Dirac spin liquid *Ansatz* and showed them to be gapless in the thermodynamic limit. By studying the energetics of states with a finite monopole density, we found no sign of an instability towards a chiral state. Our results provide further evidence that the ground state of the kagome Heisenberg antiferromagnet is well described by the Dirac spin liquid, despite having gapless monopole excitations [8]. Such a remarkable robustness was recently linked to free-fermion band topology dictating symmetry properties of monopoles [9]. Recently, a similar analysis of monopole and bilinear excitations was performed on the Dirac spin liquid on the triangular lattice [51]. The existence of gapless monopoles may provide new experimental ways to identify U(1) Dirac spin liquids and, in particular, to resolve between gapless $Z_2$ and U(1) states. Recently, a few possibilities have been suggested, e.g., via recently proposed "monopole Josephson effect" [54], which would lead to a measurable spin current, or via the coupling between monopoles and phonons [55], which would lead to a broadening/softening of certain phonon modes.

*Acknowledgements.* We thank L. Di Pietro, A. Läuchli, Urban Seifert, C. Wang, J. Knolle, J. Willsher, S. Bhattacharjee, S. Sachdev, S. Capponi, and Y.-C. He for helpful discussions. S. B. also thanks J. Colbois, R. Mishra, and S. Niu for discussions about the project. Y.I., D.P. and S.B. acknowledge financial support by the Indo-French Centre for the Promotion of Advanced Research – CEFIPRA Project No. 64T3-1. Y.I. and S.B. would like to acknowledge support from the ICTP through the Associates Programme and from the Simons Foundation through grant number 284558FY19, IIT Madras through the QuCenDiEM CoE (Project No. SP22231244CPETWOQCDHOC), the Interna-

tional Centre for Theoretical Sciences (ICTS), Bengaluru, India during a visit for participating in the program "Frustrated Metals and Insulators" (Code: ICTS/frumi2022/9). The research of Y.I. was supported in part by the National Science Foundation under Grant No. NSF PHY-1748958 during a visit to the Kavli Institute for Theoretical Physics (KITP), UC Santa Barbara, USA for participating in the program "A Quantum Universe in a Crystal: Symmetry and Topology across the Correlation Spectrum". The work of Y.I. was performed in part and completed at the Aspen Center for Physics, which is supported by National Science Foundation grant PHY-2210452. The participation of Y.I. at the Aspen Center for Physics was supported by the Simons Foundation. Y.I. and S.B. acknowledge the use of the computing resources at HPCE, IIT Madras. This work was granted access to the HPC resources of CALMIP center under the allocation 2017-P1231. This work was also supported by the TNTOP ANR-18-CE30-0026-01 grant awarded by the French Research Council.

[1] C. Lacroix, P. Mendels, and F. Mila, *Introduction to Frustrated Magnetism: Materials, Experiments, Theory* (Springer Series in Solid-State Sciences, 2011).
[2] L. Savary and L. Balents, Quantum spin liquids: a review, Rep. Prog. Phys. **80**, 016502 (2016).
[3] G. Baskaran and P. W. Anderson, Gauge theory of high-temperature superconductors and strongly correlated Fermi systems, Phys. Rev. B **37**, 580 (1988).
[4] D. P. Arovas and A. Auerbach, Functional integral theories of low-dimensional quantum Heisenberg models, Phys. Rev. B **38**, 316 (1988).
[5] I. Affleck, Z. Zou, T. Hsu, and P. W. Anderson, SU(2) gauge symmetry of the large-$U$ limit of the Hubbard model, Phys. Rev. B **38**, 745 (1988).
[6] N. Read and S. Sachdev, Spin-Peierls, valence-bond solid, and Néel ground states of low-dimensional quantum antiferromagnets, Phys. Rev. B **42**, 4568 (1990).
[7] X. Y. Xu, Y. Qi, L. Zhang, F. F. Assaad, C. Xu, and Z. Y. Meng, Monte Carlo Study of Lattice Compact Quantum Electrodynamics with Fermionic Matter: The Parent State of Quantum Phases, Phys. Rev. X **9**, 021022 (2019).
[8] X.-Y. Song, C. Wang, A. Vishwanath, and Y.-C. He, Unifying description of competing orders in two-dimensional quantum magnets, Nat. Commun. **10**, 4254 (2019).
[9] X.-Y. Song, Y.-C. He, A. Vishwanath, and C. Wang, From Spinon Band Topology to the Symmetry Quantum Numbers of Monopoles in Dirac Spin Liquids, Phys. Rev. X **10**, 011033 (2020).
[10] X.-G. Wen, Quantum orders and symmetric spin liquids, Phys. Rev. B **65**, 165113 (2002).
[11] A. Kitaev, Anyons in an exactly solved model and beyond, Ann. Phys. (Amst.) **321**, 2 (2006).
[12] A. M. Polyakov, Quark confinement and topology of gauge theories, Nucl. Phys. B **120**, 429 (1977).
[13] V. Borokhov, A. Kapustin, and X. Wu, Topological Disorder Operators in Three-Dimensional Conformal Field Theory, J. High Energy Phys. **2002** (11), 049.
[14] M. Hermele, T. Senthil, M. P. A. Fisher, P. A. Lee, N. Nagaosa, and X.-G. Wen, Stability of $U(1)$ spin liquids in two dimensions, Phys. Rev. B **70**, 214437 (2004).
[15] P. Mendels, F. Bert, M. de Vries, A. Olariu, A. Harrison, F. Duc, J. Trombe, J. Lord, A. Amato, and C. Baines, Quantum Magnetism in the Paratacamite Family: Towards an Ideal Kagomé Lattice, Phys. Rev. Lett. **98**, 077204 (2007).
[16] J. Helton, K. Matan, M. Shores, E. Nytko, B. Bartlett, Y. Yoshida, Y. Takano, A. Suslov, Y. Qiu, J.-H. Chung, D. Nocera, and Y. Lee, Spin Dynamics of the Spin-1/2 Kagome Lattice Antiferromagnet $ZnCu_3(OH)_6Cl_2$, Phys. Rev. Lett. **98**, 107204 (2007).
[17] M. de Vries, K. Kamenev, W. Kockelmann, J. Sanchez-Benitez, and A. Harrison, Magnetic Ground State of an Experimental $S = 1/2$ Kagome Antiferromagnet, Phys. Rev. Lett. **100**, 157205 (2008).
[18] M. R. Norman, Colloquium: Herbertsmithite and the search for the quantum spin liquid, Rev. Mod. Phys. **88**, 041002 (2016).
[19] S. Yan, D. A. Huse, and S. R. White, Spin-Liquid Ground State of the $S = 1/2$ Kagome Heisenberg Antiferromagnet, Science **332**, 1173 (2011).
[20] S. Depenbrock, I. McCulloch, and U. Schollwöck, Nature of the Spin-Liquid Ground State of the $S = 1/2$ Heisenberg Model on the Kagome Lattice, Phys. Rev. Lett. **109**, 067201 (2012).
[21] Y. Ran, M. Hermele, P. Lee, and X.-G. Wen, Projected-Wave-Function Study of the Spin-1/2 Heisenberg Model on the Kagomé Lattice, Phys. Rev. Lett. **98**, 117205 (2007).
[22] Y. Iqbal, F. Becca, S. Sorella, and D. Poilblanc, Gapless spin-liquid phase in the kagome spin-$\frac{1}{2}$ Heisenberg antiferromagnet, Phys. Rev. B **87**, 060405 (2013).
[23] Y.-C. He, M. Zaletel, M. Oshikawa, and F. Pollmann, Signatures of Dirac Cones in a DMRG Study of the Kagome Heisenberg Model, Phys. Rev. X **7**, 031020 (2017).
[24] H. Liao, Z. Xie, J. Chen, Z. Liu, H. Xie, R. Huang, B. Normand, and T. Xiang, Gapless Spin-Liquid Ground State in the $S = 1/2$ Kagome Antiferromagnet, Phys. Rev. Lett. **118**, 137202 (2017).
[25] M. Hering, J. Sonnenschein, Y. Iqbal, and J. Reuther, Characterization of quantum spin liquids and their spinon band structures via functional renormalization, Phys. Rev. B **99**, 100405 (2019).
[26] M. Hastings, Dirac structure, RVB, and Goldstone modes in the kagomé antiferromagnet, Phys. Rev. B **63**, 014413 (2000).
[27] J.-W. Mei, J.-Y. Chen, H. He, and X.-G. Wen, Gapped spin liquid with $\mathbb{Z}_2$ topological order for the kagome heisenberg model, Phys. Rev. B **95**, 235107 (2017).
[28] L. Messio, B. Bernu, and C. Lhuillier, Kagome Antiferromagnet: A Chiral Topological Spin Liquid?, Phys. Rev. Lett. **108**, 207204 (2012).
[29] R.-Y. Sun, H.-K. Jin, H.-H. Tu, and Y. Zhou, Possible chiral spin liquid state in the $S = 1/2$ kagome Heisenberg model (2022), arXiv:2203.07321 [cond-mat.str-el].
[30] X. G. Wen, F. Wilczek, and A. Zee, Chiral spin states and superconductivity, Phys. Rev. B **39**, 11413 (1989).
[31] V. Kalmeyer and R. B. Laughlin, Equivalence of the Resonating-Valence-Bond and Fractional Quantum Hall States, Phys. Rev. Lett. **59**, 2095 (1987).
[32] S. Bieri, C. Lhuillier, and L. Messio, Projective symmetry group classification of chiral spin liquids, Phys. Rev. B **93**, 094437 (2016).
[33] Y.-C. He, D. N. Sheng, and Y. Chen, Chiral Spin Liquid in a Frustrated Anisotropic Kagome Heisenberg Model, Phys. Rev. Lett. **112**, 137202 (2014).
[34] S.-S. Gong, W. Zhu, and D. N. Sheng, Emergent Chiral Spin Liquid: Fractional Quantum Hall Effect in a Kagome Heisenberg Model, Sci. Rep. **4**, 6317 (2014).

[35] W. Zhu, S. S. Gong, and D. N. Sheng, Chiral and critical spin liquids in a spin-$\frac{1}{2}$ kagome antiferromagnet, Phys. Rev. B **92**, 014424 (2015).

[36] K. Kumar, K. Sun, and E. Fradkin, Chiral spin liquids on the kagome lattice, Phys. Rev. B **92**, 094433 (2015).

[37] L. Messio, S. Bieri, C. Lhuillier, and B. Bernu, Chiral Spin Liquid on a Kagome Antiferromagnet Induced by the Dzyaloshinskii-Moriya Interaction, Phys. Rev. Lett. **118**, 267201 (2017).

[38] A. Wietek, A. Sterdyniak, and A. M. Läuchli, Nature of chiral spin liquids on the kagome lattice, Phys. Rev. B **92**, 125122 (2015).

[39] S.-S. Gong, W. Zhu, L. Balents, and D. N. Sheng, Global phase diagram of competing ordered and quantum spin-liquid phases on the kagome lattice, Phys. Rev. B **91**, 075112 (2015).

[40] Y.-C. He and Y. Chen, Distinct Spin Liquids and Their Transitions in Spin-$1/2$ $XXZ$ Kagome Antiferromagnets, Phys. Rev. Lett. **114**, 037201 (2015).

[41] D. Kiese, F. Ferrari, N. Astrakhantsev, N. Niggemann, P. Ghosh, T. Müller, R. Thomale, T. Neupert, J. Reuther, M. J. P. Gingras, S. Trebst, and Y. Iqbal, Pinch-points to half-moons and up in the stars: The kagome skymap, Phys. Rev. Res. **5**, L012025 (2023).

[42] F. Ferrari, S. Niu, J. Hasik, Y. Iqbal, D. Poilblanc, and F. Becca, Static and dynamical signatures of Dzyaloshinskii-Moriya interactions in the Heisenberg model on the kagome lattice, SciPost Phys. **14**, 139 (2023).

[43] L. Messio, C. Lhuillier, and G. Misguich, Time reversal symmetry breaking chiral spin liquids: Projective symmetry group approach of bosonic mean-field theories, Phys. Rev. B **87**, 125127 (2013).

[44] T. Lugan, L. D. C. Jaubert, M. Udagawa, and A. Ralko, Schwinger boson theory of the $J_1, J_2 = J_3$ kagome antiferromagnet, Phys. Rev. B **106**, L140404 (2022).

[45] S. Bieri, L. Messio, B. Bernu, and C. Lhuillier, Gapless chiral spin liquid in a kagome Heisenberg model, Phys. Rev. B **92**, 060407 (2015).

[46] F. Becca and S. Sorella, *Quantum Monte Carlo Approaches for Correlated Systems* (Cambridge University Press, 2017).

[47] E. Dupuis and W. Witczak-Krempa, Monopole hierarchy in transitions out of a Dirac spin liquid, Ann. Phys. **435**, 168496 (2021).

[48] Y.-C. He, J. Rong, and N. Su, Conformal bootstrap bounds for the $U(1)$ Dirac spin liquid and $N = 7$ Stiefel liquid, SciPost Phys. **13**, 014 (2022).

[49] D. Poilblanc, Y. Hasegawa, and T. M. Rice, Numerical study of flux phases in the t-J model, Phys. Rev. B **41**, 1949 (1990).

[50] See supplemental material.

[51] A. Wietek, S. Capponi, and A. M. Läuchli, Quantum Electrodynamics in 2+1 Dimensions as the Organizing Principle of a Triangular Lattice Antiferromagnet (2023), arXiv:2303.01585 [cond-mat.str-el].

[52] I. Affleck and J. B. Marston, Large-n limit of the Heisenberg-Hubbard model: Implications for high-$T_c$ superconductors, Phys. Rev. B **37**, 3774 (1988).

[53] Y. Iqbal, D. Poilblanc, and F. Becca, Vanishing spin gap in a competing spin-liquid phase in the kagome Heisenberg antiferromagnet, Phys. Rev. B **89**, 020407 (2014).

[54] G. Nambiar, D. Bulmash, and V. Galitski, Monopole Josephson effects in a Dirac spin liquid, Phys. Rev. Res. **5**, 013169 (2023).

[55] U. F. P. Seifert, J. Willsher, M. Drescher, F. Pollmann, and J. Knolle, Spin-Peierls instability of the $U(1)$ Dirac spin liquid (2023), arXiv:2307.12295 [cond-mat.str-el].

[56] A. M. Läuchli, J. Sudan, and R. Moessner, $s = \frac{1}{2}$ kagome heisenberg antiferromagnet revisited, Phys. Rev. B **100**, 155142 (2019).